

# Organic Molecule Ejection from Surfaces due to Heavy Particle Bombardment

Barbara J. Garrison<sup>†</sup>

Contribution from the Department of Chemistry, The Pennsylvania State University, University Park, Pennsylvania 16802. Received March 2, 1982

**Abstract:** Classical dynamics calculations have been performed for a model system of energetic Ar particles bombarding a  $c(4 \times 4)$  ordered overlayer of benzene on Ni(001). We find the predicted mass spectrum of ejected particles to be dominated by the parent molecule  $C_6H_6$ , in agreement with experimental results. Our estimate of the internal vibrational energy of the ejected benzene molecules indicates that the majority of the molecules will not fragment during their flight to the detector. The mass spectrum of the desorbed benzene molecules and fragments is sensitive to the bonding and orientation of the molecules in the original sample. The predicted fragment distribution is quite different in calculations where the benzene molecule is originally flat on the surface and when the molecule is originally standing up, as for the case of pyridine.

The application of energetic ion and atom beams to the analysis of nonvolatile, high molecular weight compounds is a rapidly evolving research field.<sup>1</sup> In traditional mass spectrometry a molecule is usually volatilized by heating and then ionized by electron impact. For molecules like amino acids, small peptides, and nucleotides, however, heating usually leads to thermal decomposition whereas ion or atom bombardment may directly produce the desired molecular ion. In other words, the sub-picosecond time scale of the impact event is sufficiently fast to beat out thermal rearrangements that occur on the nanosecond time scale. This field of organic secondary ion mass spectrometry (SIMS) was originally developed by Benninghoven using ion beams.<sup>2</sup> Another recent approach has been to employ an atom beam rather than an ion beam as the bombarding species.<sup>3</sup> The workers using this experimental configuration have termed the technique FAB, or fast atom bombardment, rather than SIMS. Although there are operational differences in the two experimental setups, the fundamental processes controlling the ejection of atoms and molecules from the surface should be identical.

Typically the primary particle, either atom or ion, initially has several hundred to a few thousand electronvolts of kinetic energy. Bombardment of an organic sample with this highly energetic particle would appear to be quite destructive. However, the parent ion, the parent ion  $\pm$  one proton, or a cationized parent molecule is usually observed, oftentimes as the most intense peak.<sup>4,5</sup> In a previous study we examined for the first time the possible nuclear motion in the solid that can lead to the ejection of the molecular and fragmented species.<sup>6</sup> The classical dynamics procedure used to determine mechanisms of ejection can also be used to probe other experimental observables, such as energy and angular distributions of the ejected particles. In this paper we describe in more detail the classical dynamics procedure used in the organic molecule studies and present a number of calculated results that may be compared with experiment. We feel that a study of this type is needed now because there is considerable experimental work going on in the field and the classical dynamics procedure yields an atomic and molecular basis for understanding the many observables. This fundamental understanding can then be a useful guide in selecting suitable experimental conditions to enhance observables of interest, for example, molecular desorption.

The model system studied is benzene,  $C_6H_6$ , which adsorbs in an ordered  $c(4 \times 4)$  overlayer on Ni(001).<sup>7,8</sup> This system was chosen for several reasons. First, it adsorbs in an ordered overlayer on Ni(001) at room temperature. Second, benzene is larger than the types of molecules theoretically modeled to date yet is simple enough to handle computationally. Third, a sufficient number of Ar impacts can be calculated so that the predicted observables can be compared with those obtained from a variety of experimental techniques. Finally, the effect of bonding geometry on the desorption process can be examined by standing the molecule

upright on the surface. This is the geometry of pyridine on a metal surface.

The results show that the calculated mass spectrum is dominated by the parent molecule,  $C_6H_6$ . An estimate of the internal energy of these molecules indicates that  $\sim 75\%$  of them have less than 5 eV of energy. This implies that there will not be significant fragmentation of the parent molecule during the flight to the detector. The energy distribution for the  $C_6H_6$  molecules peaks at low energies (1–2 eV) and terminates at  $\sim 12$  eV. We find best agreement between the experimental energy distributions<sup>9</sup> for  $Ni^+$  and  $NiC_6H_6^+$  and the respective calculated ones if we adjust the calculated distributions for the image force that an ejecting ion must experience.<sup>10</sup> The benzene molecules tend to eject in a more normal direction from the surface than the Ni atoms. In contrast to other systems studied, very little azimuthal angular dependence of the ejected benzene molecules is found. The bonding geometry of the molecule, either lying down as in the case of benzene or standing up as in pyridine, strongly influences the ejection process. There is more fragmentation and less molecular ejection in the case of pyridine on Ni(001) than for benzene. This result implies that the nature of the fragmentation should be strongly matrix dependent.

## Description of the Calculation

The nickel–benzene system has been modeled by a classical dynamics procedure that was developed over the past few years to study in detail the bombardment process and subsequent ejection of particles.<sup>11–17</sup> Briefly, the theoretical model consists of ap-

- (1) B. J. Garrison and N. Winograd, *Science (Washington, D.C.)*, **216**, 805 (1982).
- (2) A. Benninghoven, *Surf. Sci.*, **53**, 596 (1975).
- (3) M. Barber, R. S. Bardoli, R. D. Sedgewick, and A. N. Tyler, *J. Chem. Soc., Chem. Commun.*, 325 (1981).
- (4) A. Benninghoven, D. Jaspers, and W. Sichtermann, *Appl. Phys.*, **11**, 35 (1976).
- (5) H. Grade, N. Winograd, and R. G. Cooks, *J. Am. Chem. Soc.*, **99**, 7725 (1977).
- (6) B. J. Garrison, *J. Am. Chem. Soc.*, **102**, 6553 (1981).
- (7) J. C. Bertolini, G. Dalmai-Imelik, and J. Rousseau, *Surf. Sci.*, **67**, 478 (1977).
- (8) J. C. Bertolini and J. Rousseau, *Surf. Sci.*, **89**, 467 (1979).
- (9) E. J. Karwacki and N. Winograd, to be published.
- (10) R. A. Gibbs, S. P. Holland, K. E. Foley, B. J. Garrison, and N. Winograd, *Phys. Rev. [Sect.] B*, **24**, 6178 (1981); *J. Chem. Phys.*, **76**, 684 (1982).
- (11) B. J. Garrison, N. Winograd, and D. E. Harrison, Jr., *J. Chem. Phys.*, **69**, 1440 (1978).
- (12) N. Winograd, D. E. Harrison, Jr., and B. J. Garrison, *Surf. Sci.*, **78**, 467 (1978).
- (13) B. J. Garrison, N. Winograd, and D. E. Harrison, Jr., *Phys. Rev. [Sect.] B*, **18**, 6000 (1978).
- (14) B. J. Garrison, N. Winograd, and D. E. Harrison, Jr., *J. Vac. Sci. Technol.*, **16**, 789 (1979).

<sup>†</sup> Alfred P. Sloan Fellow.

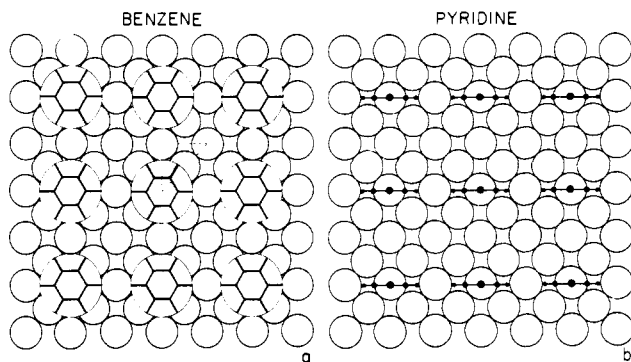


Figure 1. Placement of atoms. (a) Ni(001) with  $c(4 \times 4)$  overlayer of benzene,  $C_6H_6$ . The dashed triangle is the impact zone for normal incidence bombardment. The circle around each benzene is the radical extent of the hydrogen position, 2.5 Å. (b) Ni(001) with a  $c(4 \times 4)$  overlayer of pyridine. The dashed square is the impact zone for normal incidence bombardment.

proximating the solid by a finite microcrystallite. In this case the Ni(001) crystal has three layers of 85 atoms per layer. Nine benzene molecules are then placed on the surface in a  $c(4 \times 4)$  configuration (Figure 1a). Assuming a pairwise interaction potential among all the atoms, Hamilton's equations of motion are integrated to yield the positions and momenta of all particles—the primary Ar particle, the substrate Ni atoms, and adsorbate atoms in the benzene molecule—as a function of time during the collision cascade. The final positions and momenta can be correlated with observables such as total yield of ejected particles, energy distributions, angular distributions, and possible cluster formation.<sup>11-14,17</sup>

To determine the forces between the atoms, we assume the interaction potential to be pairwise additive. In a molecule such as benzene, care must be taken to distinguish among the various pairs of atoms. For example, carbon atoms that are closest neighbors in the molecule will experience a different interaction than carbon atoms on opposite sides of the ring or even in separate molecules. For simplicity we choose to use only two different potentials for any given mass pair of atoms. That is, we use a bonding and a nonbonding carbon-carbon interaction potential, a bonding and a nonbonding carbon-hydrogen interaction, and only a nonbonding hydrogen-hydrogen interaction potential. Several assumptions are made regarding these interactions. Both the bonding and nonbonding interactions depend only on the distance between two atoms; thus bond bending type interactions are neglected. This pairwise sum of interaction potentials does not properly describe the various rearrangement channels that the benzene could undergo after it has been collisionally excited during the bombardment process. The neglect of these more accurate interactions should not affect the basic mechanisms of ejection of the benzene molecule itself. Their neglect, however, means that examining the absolute fragmentation probabilities is outside the scope of this study. We have made preliminary calculations with the inclusion of bond-bending forces and found them to have little effect on ejection mechanisms and probabilities, although the internal energy and final geometry of the benzene is affected.<sup>18</sup>

The carbon and hydrogen interactions are assumed to have the functional form of a Morse potential:

$$V = D_e e^{-\beta(R-R_e)} (e^{-\beta(R-R_e)} - 2) \quad R \leq R_c \quad (1a)$$

$$V = 0 \quad R > R_c \quad (1b)$$

where  $R$  is the distance between the pair of atoms. Most of the

Table I. Potential Parameters

	$D_e$ , eV	$\beta$ , Å <sup>-1</sup>	$R_e$ , Å	$R_c$ , Å
C-C (bonding)	5.00	2.25	1.39	4.22
C-H (bonding)	4.28	1.83	1.11	4.22
C-C (nonbonding)	0.0022	1.60	3.88	4.22
C-H (nonbonding)	0.0023	1.80	3.44	4.22
H-H (nonbonding)	0.0024	2.05	3.00	4.22
Ni-H	0.013	2.70	2.03	4.22
Ni-C (benzene)	0.085	2.26	2.41	4.22
Ni-C (pyridine)	0.82	2.45	1.76	4.22

parameters are adapted from those used by Allinger in his Molecular Mechanics II (MMII) program.<sup>19</sup> The C-C values for benzene are assumed to be an average of the values for carbon single and double bonds. The values of the parameter  $\beta$  are determined by assuming that the force constant of the Morse potential at  $R = R_c$  (equilibrium separation) is the same as the force constant used in MMII.

Since the bonding interactions are quite strong ( $D_e \sim 4-5$  eV), the same potentials for the non-nearest-neighbor atoms cannot be used since the molecule would be too tightly bound together. These interactions must not be neglected, however, since the repulsive force becomes important at small values of internuclear distances. A Morse potential is fit to the van der Waals interaction that is used in MMII to alleviate this problem. The nonbonding potentials are used for all interactions between atoms that are *not* nearest neighbors in the original configuration of benzene molecules on the surface. All the potential parameters are given in Table I. This procedure of using separate bonding and nonbonding potential pairs is the same as was used for the study of carbon monoxide adsorbed on the various crystal faces of nickel.<sup>17,20</sup>

For the Ni-C and Ni-H interactions we first assume a specific geometry of the benzene overlayer structure. The placement of the  $C_6H_6$  molecule with respect to the Ni atom is not precisely known, but it is generally agreed that the ring is parallel to the surface.<sup>7,8,21</sup> The  $\pi$ -bonded site with the  $C_6H_6$  molecule placed on top of a nickel atom is consistent with current electron energy loss spectra.<sup>7,8</sup> The exact placement of the molecule on the surface, however, is not known. Using the geometry parameters from theoretical calculations of nickel-ethylene complexes,<sup>22</sup> we arbitrarily place the benzene 1.96 Å above the nickel atom. With this geometry  $R_c$  of eq 1 was determined to be the distance from the carbon or hydrogen atom to the nearest surface Ni atom. The values of  $D_e$  are adjusted to give a total binding energy of 1.7 eV.<sup>23</sup> Most of the interaction is thought to be through the Ni-C bonds rather than the Ni-H bonds; thus we arbitrarily divide the interactions in this fashion. The values of  $\beta$  are chosen to give a reasonable repulsion at small internuclear separations. The values of  $\beta$  and  $D_e$  are varied to test their influence on the ejection process.

Two functional forms for the Ar-Ni, Ar-C, and Ar-H potentials are examined in this study. The first form is an exponential repulsion or Born-Mayer form where

$$V = Ae^{-BR} \quad R \leq R_a \quad (2b)$$

$$V = 0 \quad R > R_a \quad (2b)$$

and is the potential that has been employed in most of our previous studies.<sup>13,17</sup> The values of  $A$  are 68.84, 14.75, and 2.46 keV for Ar-Ni, Ar-C, and Ar-H, respectively, and the value of  $B$  is fixed at 4.593 Å<sup>-1</sup>. These potentials are plotted in Figure 2.

(15) D. E. Harrison, Jr., P. W. Kelly, B. J. Garrison, and N. Winograd, *Surf. Sci.*, **76**, 311 (1978).

(16) N. Winograd, B. J. Garrison, T. Fleisch, W. N. Delgass, and D. E. Harrison, Jr., *J. Vac. Sci. Technol.*, **16**, 629 (1979).

(17) N. Winograd, B. J. Garrison, and D. E. Harrison, Jr., *J. Chem. Phys.*, **73**, 3473 (1980).

(18) B. J. Garrison, to be published.

(19) N. L. Allinger and J. T. Sprague, *J. Am. Chem. Soc.*, **95**, 3893 (1973); N. L. Allinger, *ibid.*, **99**, 8127 (1977).

(20) K. E. Foley and N. Winograd, *Surf. Sci.*, in press; K. E. Foley, Ph.D. Thesis, Purdue University, 1981.

(21) S. Lehwald, H. Ibach, and J. E. Demuth, *Surf. Sci.*, **78**, 577 (1978), and references therein.

(22) (a) T. H. Upton and W. A. Goddard, III, *J. Am. Chem. Soc.*, **100**, 322 (1978); (b) G. A. Ozin, W. J. Power, T. H. Upton, and W. A. Goddard, III, *ibid.*, **100**, 4750 (1978).

(23) J. G. Demuth and D. E. Eastman, *Phys. Rev. Lett.*, **32**, 1123 (1974).

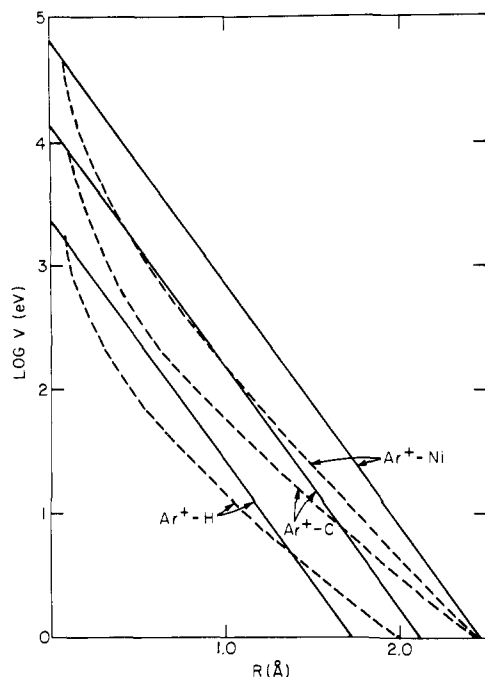


Figure 2. Ar potentials: (—) Born-Mayer; (---) Moliere.

The second potential to describe the Ar-substrate interaction is the Moliere form,<sup>24</sup> where

$$V = \frac{Z_1 Z_2 e^2}{R} (0.35e^{-0.3R/a} + 0.55e^{-1.2R/a} + 0.10e^{-6.0R/a}) \quad R \leq R_a \quad (3a)$$

$$V = 0 \quad R > R_a \quad (3b)$$

with the screening length  $a$  given by

$$a = 0.885a_0(Z_1^{1/2} + Z_2^{1/2})^{-2/3} \quad (4)$$

where  $Z_1$ ,  $Z_2$  are the atomic numbers of the two atoms, and  $a_0$  is the Bohr radius (0.529 Å). As shown in Figure 2, the Moliere potentials for the Ar-Ni, Ar-C, and Ar-H interactions correspond to smaller atom sizes at a given energy than the Born-Mayer functions. These two forms of the Ar interactions span a considerable range for the possible values of the potential. Certainly the differences between the Ar<sup>+</sup> ion-surface and the Ar neutral-surface interactions are not this large. Thus, we believe that any similar conclusions that are drawn from both forms of the potential should be appropriate for either Ar<sup>0</sup> or Ar<sup>+</sup> bombardment experiments. The Ni-Ni interaction is the same as we have used previously in our studies of CO adsorbed on Ni(001). The potential form and parameters are given in ref 17.

The primary ion must bombard at all unique points on the surface to properly reproduce experimental results. Assuming benzene is circular rather than having sixfold symmetry, the appropriate impact zone for normal incidence bombardment is shown in Figure 1a. This zone is already 8 times larger than the one for the clean metal. For the studies presented here, 55 Ar impacts within this zone are sampled. In one case, 820 impacts of the primary particle are calculated. These results are used to predict the energy and angular distributions since more ejected particles are needed to obtain statistically reliable distributions.

For the pyridine adsorption at high coverages on silver, it is proposed that the bonding occurs through the nitrogen lone pair as a  $\sigma$  bond<sup>25</sup> rather than a  $\pi$  bond as for benzene. Under these conditions, the plane of the molecule is thought to approach an orientation perpendicular to the surface. In our model calculations,

then, the pyridine is arbitrarily placed in an atop or linearly bonded site above a nickel atom standing straight up with the nitrogen 1.76 Å above the surface plane. This is the same height and site symmetry as for CO on Ni(001).<sup>17</sup> We also employed the same Ni-C potential as for the CO studies.<sup>17</sup> These interactions result in a binding energy for the pyridine to the surface of 1.8 eV. The potential parameters are given in Table I. The nitrogen atom is assumed to have the same mass and interaction potentials as the carbon atom. There should not be large differences between the two atoms in the scattering process. In addition, this replacement allows straightforward comparisons between pyridine and benzene trajectories. The placement of atoms as well as the impact zone are shown in Figure 1b.

## Results and Discussion

The calculations predict that benzene molecules eject intact. The mechanistic reasons for the molecular ejection are discussed in a previous paper.<sup>6</sup> Briefly summarized, these include the facts that (i) the energy of the primary particle is rapidly dissipated to energies of the order of chemical bond strengths by multiple collisions in the solid, (ii) there are many internal vibrational modes that can absorb excess energy from a violent collision, and (iii) multiple carbon atoms can be struck by a larger substrate atom, forcing them to move in a concerted fashion and not fragment the molecule. In addition to the molecular benzene, a number of hydrocarbon fragments are observed. We also predict metal benzene clusters Ni<sub>n</sub>C<sub>6</sub>H<sub>6</sub> where  $n = 1-4$ , as well as occasional complexes such as NiC<sub>4</sub>H<sub>4</sub>, NiC<sub>3</sub>H<sub>5</sub>, or NiC<sub>6</sub>H<sub>5</sub>.

In the following sections we will discuss the mass spectra of the ejected benzene molecule and fragments as well as the effect of the primary ion energy, interaction potentials, and the bonding geometry of the benzene to the surface on the predicted yields and fragmentation processes.

**Comparison of Mass Spectra.** The calculated mass spectrum for the Ar bombardment at 1 keV is shown in Figure 3a. The intensities are normalized to the C<sub>6</sub>H<sub>6</sub> peak with only those species whose intensities are at least 5% of the C<sub>6</sub>H<sub>6</sub> peak being shown. The hydrocarbon fragments are predominantly characterized by equal numbers of carbon and hydrogen atoms although the parent species is by far the most intense. Due to the interaction potentials used, the number of carbon atoms in a fragment must always be greater than or equal to the number of hydrogen atoms. This spectrum has not been corrected for the probability of the species becoming ions during ejection, the stability of a fragment (e.g., C<sub>5</sub>H<sub>5</sub> is not stable), or the possible further fragmentation of the larger species on the way to the detector. This spectrum also includes all fragments that eject from each benzene molecule. Thus, if a molecule is broken into six CH diatomics, all six fragments are theoretically counted. Obviously this overestimates the intensity of the smaller fragments. Besides the species indicated in the spectrum, the calculations predict clusters of the types C<sub>k</sub>H<sub>m</sub>, NiC<sub>n</sub>H<sub>m</sub>, Ni<sub>k</sub>C<sub>n</sub>H<sub>m</sub>, and Ni<sub>k</sub>(C<sub>6</sub>H<sub>6</sub>)<sub>2</sub>, where  $k < 4$  and  $m < n \leq 6$ . As discussed below, the mass spectrum calculated from using the Born-Mayer Ar potentials is very similar to that shown in Figure 3a.

An analysis of the internal vibrational energy of the ejected C<sub>6</sub>H<sub>6</sub> molecules indicates that there will not be a significant amount of fragmentation. The median vibrational energy is ~2.5 eV, with ~75% of the molecules having less than 5 eV. These energies are less than or equal to the C-H bond strength (4.28 eV) and the C-C bond strength (5.00 eV). This much energy, however, in an unstable species such as C<sub>5</sub>H<sub>5</sub> will undoubtedly cause it to rearrange or fragment further. It should be possible to experimentally measure the vibrational populations of these excited molecules.

It is worthwhile to compare this calculated spectrum with those produced from a variety of experimental techniques. Recently Karwacki and Winograd obtained the SIMS spectrum for Ni(001) exposed to 3 langmuirs (1 langmuir = 10<sup>-6</sup> torr-s) of benzene.<sup>9</sup> This dose corresponds approximately to that required to form the c(4 × 4) structure. Their spectrum contains only Ni<sup>+</sup>, Ni<sub>2</sub><sup>+</sup>, and NiC<sub>6</sub>H<sub>6</sub><sup>+</sup> peaks and is shown in Figure 3b. In both cases the Ni

(24) I. M. Torrens, "Interatomic Potentials", Academic Press, New York, 1972.

(25) J. E. Demuth, P. N. Sanda, J. M. Warlaumont, J. C. Tsang, and K. Christman in "Proceedings of the Second International Conference on Surface Vibrations", North-Holland, Amsterdam, 1980.

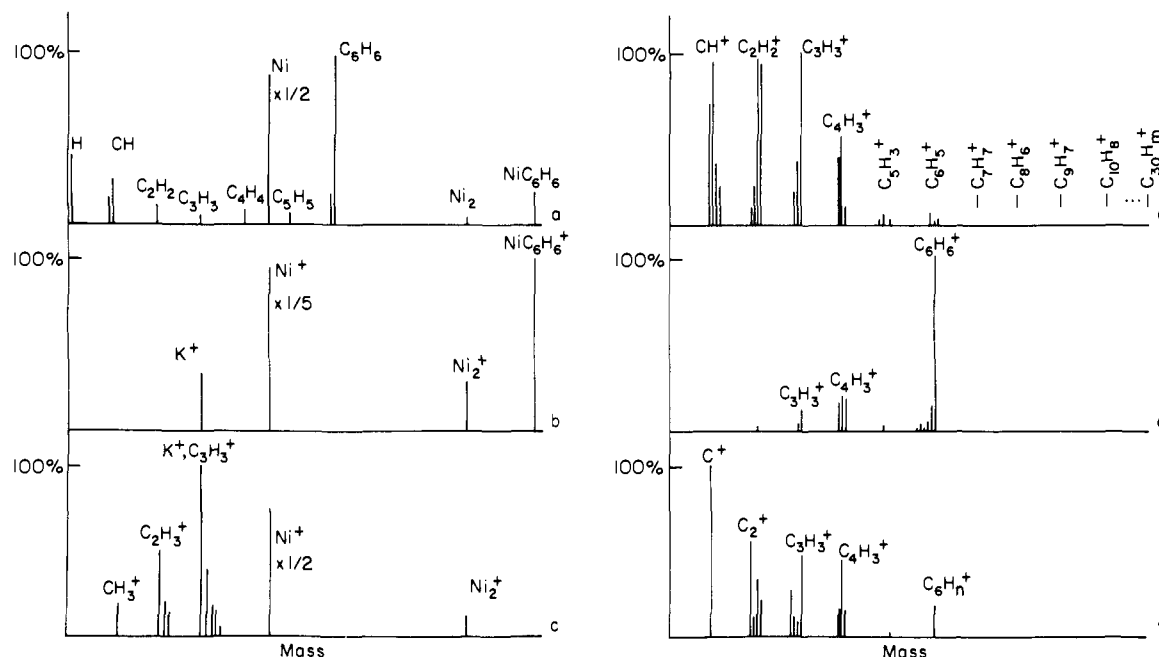
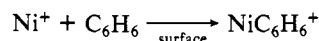


Figure 3. Benzene mass spectra. The most intense peak in each grouping has been identified. (a) Calculated, Ar with 1000 eV, Moliere potential. (b) Experimental SIMS, 3 langmuirs of  $C_6H_6$  on Ni(001), ref 9. (c) Experimental SIMS, 2100 langmuirs of  $C_6H_6$  on Ni(001), ref 9. (d) Experimental SIMS, solid benzene, ref 26. (e) Electron impact, ref 28. (f) Resonance-enhanced multiphoton ionization, ref 29, Figure 9.

peak dominates. The predominant organic species in each spectrum contains the parent molecule— $C_6H_6$  in the calculations and  $NiC_6H_6^+$  in the experiment—rather than a hydrocarbon fragment. From previous studies of CO on nickel<sup>17</sup> and this study of  $C_6H_6$  on nickel, we believe these cationized species form via reactions of the type



where the surface may participate in the energy transfer and ionization process. Thus the charge is related to the ionization potential of Ni (7.6 eV) rather than to that of benzene (9.2 eV). Apparently the ionization potential of benzene is too high for  $C_6H_6^+$  to be formed. In agreement with the calculations, negligible fragmentation is detected in this experiment.<sup>9</sup>

Karwacki and Winograd also performed SIMS experiments for  $C_6H_6$  adsorbed on Ni(001) where they dosed the surface with 2100 langmuirs of benzene.<sup>9</sup> This SIMS spectrum is shown in Figure 3c. Here the multiple layers of benzene attenuate the  $Ni^+$  peak, and the cationized  $NiC_6H_6^+$  peak completely disappears. This spectrum, however, does contain hydrocarbon fragments of lower masses.

Two SIMS experiments have been performed on solid benzene at a temperature of 77 K.<sup>26,27</sup> The low mass spectrum from Lancaster et al. is shown in Figure 3d. They observe peaks at all masses corresponding to  $C_nH_m^+$  where  $n \leq 30$ . The predominant peaks are the  $C_1$ ,  $C_2$ , and  $C_3$  species, in agreement with the work of Karwacki and Winograd (Figure 3c). We believe the reason we do not observe these  $C_nH_m^+$  species with  $n > 6$  in the calculations is due to the low density of benzene molecules on the Ni surface.

It is obvious from Figure 3b–d that the sample preparation strongly affects the mass spectrum. The low coverage study appears to be the one where the parent species can be most easily identified as long as there is an energetically favorable means of ionization, e.g., cationization. The solid benzene studies are interesting in that a variety of large clusters are observed. However, if the sample were of an unknown compound, it would be difficult to extract the parent species from Figure 3d.

Two other means of ionization, electron impact and resonance-enhanced multiphoton ionization (REMPI), produce spectra as shown in Figure 3e,f. Both spectra are different from the previous ones discussed. The electron-impact spectrum (Figure 3e) shows predominantly  $C_6H_6^+$  species but with significant amounts of  $C_4$  and  $C_3$  fragments.<sup>28</sup> The REMPI spectrum (Figure 3f) is dominated by the  $C^+$  fragment.<sup>29</sup> Recent work has indicated that the extensive fragmentation in the REMPI spectrum is due to absorption of photons by larger fragments of the benzene causing further dissociation.<sup>30</sup> This mechanism is in contrast to one where many photons are pumped directly into the vibrational modes of  $C_6H_6$ .

**Effect of the Primary Energy and the Ar Potentials.** It has been suggested that as the primary particle energy increases the ratio of the yield of fragmented molecules to the yield of molecular species decreases.<sup>31</sup> The rationale for this hypothesis is that the fragmented species should only arise from direct collisions with the primary particle; thus the yield of fragments should be relatively constant with primary particle energy. The yield of molecular species, however, should increase with primary ion energy. In these calculations we find that both molecular ejection and ejection with fragmentation increase with the primary ion energy and that their ratio is relatively constant. This conclusion is also borne out by calculations of the effect of the primary ion energy on the ratio of the dissociative to molecular ejection of CO from a CO-covered nickel surface.<sup>20</sup>

The yields of Ni atom and molecular species ejected as a function of primary particle energy are shown in Figure 4a,b. For this figure we have combined the yields from all species with six carbons, i.e.,  $C_6H_6$ ,  $C_6H_5$ ,  $Ni_nC_6H_6$ , and  $Ni_nC_6H_5$ . Over the energy range studied, 100–1500 eV, both yields increase with increasing energy. In Figure 4c is plotted the ratio of the yield of the CH fragment to the yield of the  $C_6$  species. This ratio is virtually constant over the energy range studied. Several definitions of fragmented yield were tried and the same conclusions were reached. At the low energies (100 and 200 eV), all the

(28) Selected Mass Spectral Data, Serial No. 250, Thermodynamics Research Center, AP144 Hydrocarbon Project, Thermodynamics Research Center, Texas A&M University, College Station, TX.

(29) L. Zandee and R. B. Bernstein, *J. Chem. Phys.*, **71**, 1359 (1979).

(30) U. Boesl, H. J. Neusser, and E. W. Schlag, *J. Chem. Phys.*, **72**, 4327 (1980).

(31) M. Barber, J. C. Vickerman, and J. Wolstenholme, *J. Chem. Soc., Faraday Trans. 1*, **76**, 549 (1980).

(26) G. M. Lancaster, F. Honda, Y. Fukuda, and J. W. Rabalais, *J. Am. Chem. Soc.*, **101**, 1951 (1979).

(27) H. T. Jonkman, J. Michl, R. N. King, and J. D. Andrade, *Anal. Chem.*, **50**, 2078 (1978).

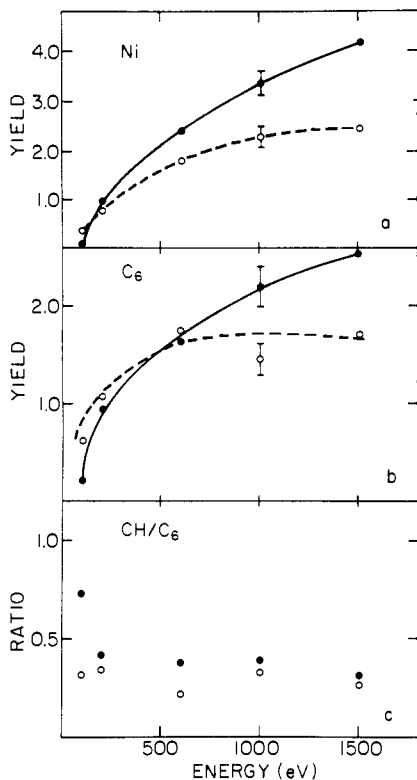


Figure 4. Yields vs. primary ions energy: (—●—) Born-Mayer; (---○---) Moliere.

fragmented species arise from the Ar directly striking the central benzene of Figure 1a. As the energy increases, not only is there dissociation of the target benzene, but some of the Ni atoms and energetic carbon fragments have sufficient energy to break up other benzene molecules.

The effect of the Ar potentials, Born-Mayer vs. Moliere, is also displayed in Figure 4. For both the Ni and C<sub>6</sub> yields, the results from the two potentials are comparable at the low primary ion energies, but the Moliere potential gives lower yields at the higher energies. These results are similar to those from studies on clean metals.<sup>32</sup> Although the absolute yields can differ significantly with the two potentials, the ratio of CH yield to C<sub>6</sub> yield is very similar. The only point in real discrepancy is at 100 eV with the Born-Mayer potential. This is due to the extremely low yield of C<sub>6</sub> species (Figure 4b). The calculations do not predict any relative decrease in fragmentation probability as the primary energy increases.

The Born-Mayer and Moliere potentials for the Ar interactions are quite different, as seen in Figure 2. Consequently, each predicts different yields of species ejecting from the solid. However, the overall mass spectrum is very similar; e.g., the CH/C<sub>6</sub> ratio is virtually identical for both potentials.

**Effect of the Ni-C Potential.** One of the mechanistic reasons for the intact ejection of benzene molecules is that one nickel atom simultaneously or sequentially strikes several carbon atoms, forcing the molecule as a whole to move in one direction. This argument is based on the fact that the nickel atom is larger than the carbon atom. Note in Figure 1a that the carbon ring of the benzene molecule has essentially the same diameter as the Ni atom. This relative size is controlled by the Morse parameter  $\beta$  of the Ni-C interaction potential (eq 1a). As  $\beta$  increases, the relative size of the two atoms increases. Shown in Figure 5 are the C<sub>6</sub> and CH yields as well as the CH/C<sub>6</sub> ratio as a function of  $\beta$  of the Ni-C interaction. The yields are virtually independent of the size of the atoms as described by  $\beta$ . Thus we conclude that the mechanisms of ejection are relatively insensitive to this parameter. It is also possible to test the influence of  $D_e$  on the various ejection yields. By increasing  $D_e$  such that the surface binding energy is

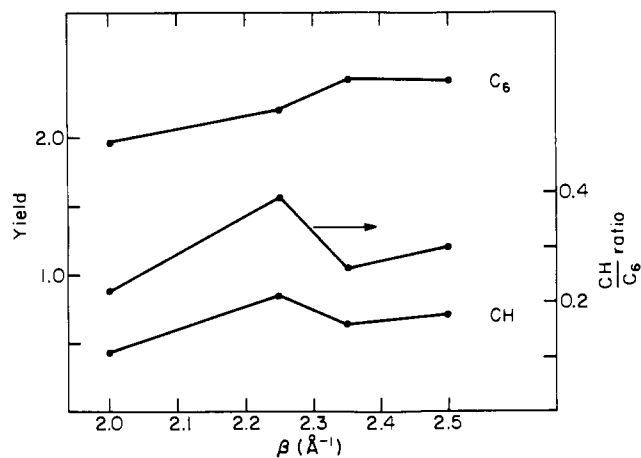


Figure 5. Yields vs. Morse parameter,  $\beta$ . The Born-Mayer potential was used for the Ar interactions. The Ar initially had 1000 eV of energy.

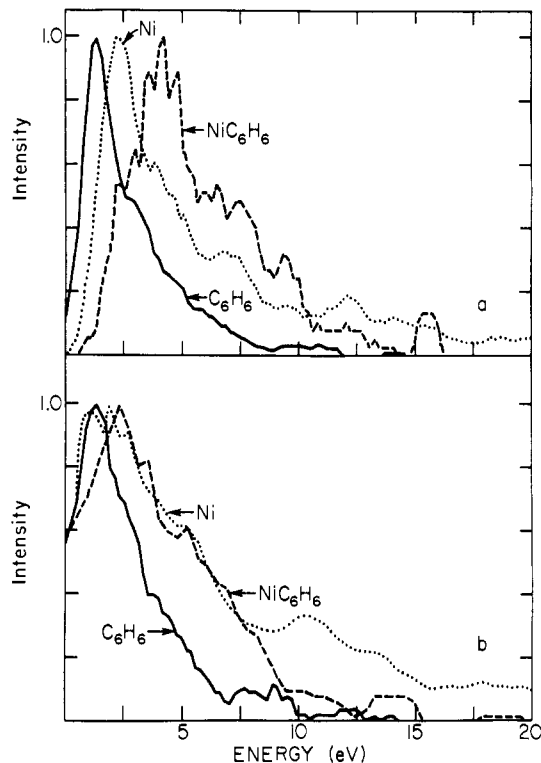


Figure 6. Energy distributions. The results are from the calculation using the Moliere potential with the Ar having 1000 eV of energy. A total of 820 impact points were calculated. (a) Uncorrected distributions. (b) Distributions corrected for a 1.8-eV image force (ref 10).

3.6 eV rather than 1.7 eV, we find that the molecular yield decreases by 30%. This result is in qualitative agreement with other studies that indicate that the yield is roughly inversely proportional to  $D_e$ . In addition, however, the results indicate that the degree of fragmentation is rather insensitive to surface binding energy. The reason for this observation is that collisions required to fragment the molecule are usually significantly larger than the surface binding forces. In contrast, the softer collisions that lead to molecular desorption are on the order of binding energy, and these collisions are obviously more sensitive to the value of this attractive energy.

**Energy and Angular Distributions.** The angular distributions of ejected atoms and small molecules have been shown to reflect their original local bonding geometry.<sup>10,33-36</sup> This is particularly

(32) N. Winograd, D. E. Harrison, Jr., unpublished results.

(33) N. Winograd, B. J. Garrison, and D. E. Harrison, Jr., *Phys. Rev. Lett.*, **41**, 1120 (1978).

(34) S. P. Holland, B. J. Garrison, and N. Winograd, *Phys. Rev. Lett.*, **43**, 220 (1979).

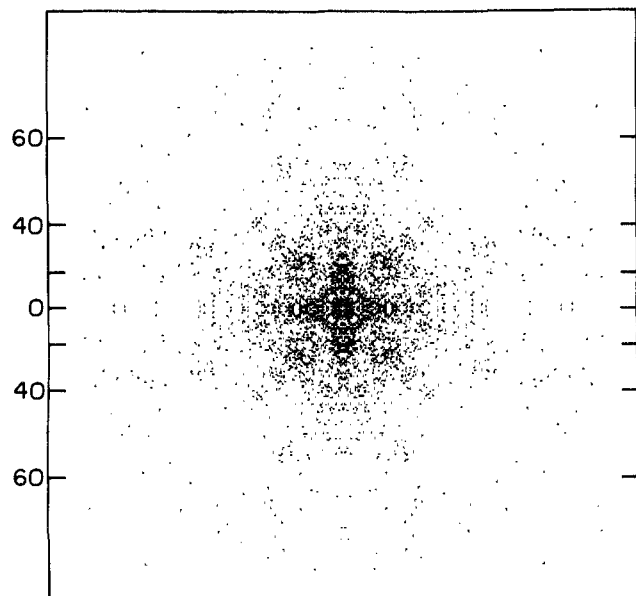


**Figure 7.** Angular distribution of the ejected benzene molecules. Only those particles with greater than 2 eV of kinetic energy are shown. Each ejected molecule is plotted on a flat-plate collector an arbitrary distance above the crystal. The numbers on the ordinate refer to the polar deflection angle given in degrees. The plate is oriented the same as the crystal in Figure 1a.

valid for the high energy ejected particles which leave early in the collision cascade before significant surface damage has occurred. In contrast to even the ejection of molecular carbon monoxide,<sup>17</sup> the benzene molecules tend to eject with much lower energies and without any real preferred azimuthal direction. Shown in Figure 6 is the center of mass kinetic energy distribution of ejected benzene molecules, Ni atoms, and NiC<sub>6</sub>H<sub>6</sub> clusters from the calculation with Ar at 1000 eV using the Moliere potential. For this case 820 impacts were calculated with over 1000 C<sub>6</sub>H<sub>6</sub> species ejecting. These distributions are typical of those at other Ar energies.

The benzene distribution peaks at ~1 eV and terminates at about 12 eV. The atomic Ni distribution, however, has a high-energy tail that extends to about 100 eV. For CO molecules ~10% of the ejected intact molecules have energies above 15 eV. It appears that an energetic collision that would eject the benzene molecule with high kinetic energy leads instead to fragmentation. The energy distributions of C<sub>3</sub>H<sub>3</sub> and especially C<sub>2</sub>H<sub>2</sub> are broader and exhibit a higher energy tail. There appears to be a correlation between the fragmentation process and the final kinetic energies of the species.

Preliminary examination of the angular distribution of the ejected C<sub>6</sub>H<sub>6</sub> molecules indicates that the direction of desorption is not strongly affected by the underlying crystal symmetry. The angular distribution of the C<sub>6</sub>H<sub>6</sub> molecules with greater than 2 eV of kinetic energy is shown in Figure 7 as a spot pattern. Although there does appear to be preferred directions for ejection, the anisotropy is not nearly as great as for the substrate atom or even atomic adsorbates.<sup>10,33-36</sup> There is still some possibility that the benzene distributions will reflect the bonding-site symmetry, e.g., atop vs. fourfold bridged site, as was the case for the atomic adsorbates, but these preliminary results do not appear favorable for such an analysis.

As is apparent from Figure 7, the C<sub>6</sub>H<sub>6</sub> molecules tend to eject in a direction normal to the surface. The polar angle distributions of the C<sub>6</sub>H<sub>6</sub> molecules, Ni atoms, and NiC<sub>6</sub>H<sub>6</sub> clusters are shown in Figure 8. Here the angle  $\theta$  is measured from the surface normal. The Ni atom distribution is similar to those observed

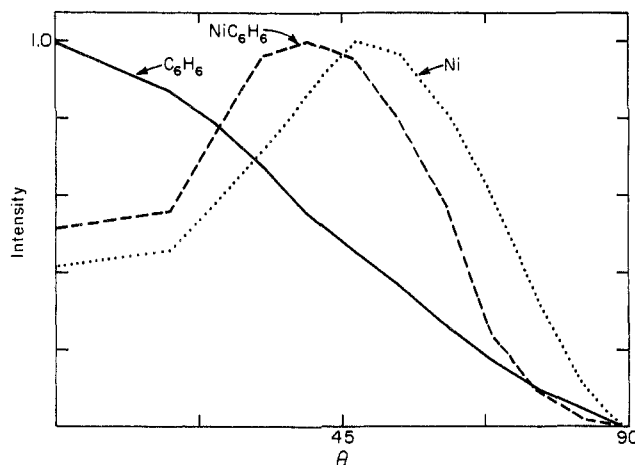


**Figure 8.** Polar angle distributions. The azimuthal angle of collection is along the (100) direction (horizontal or vertical in Figures 1 and 7). The same calculation as described in the caption to Figure 6 is used. The polar resolution is  $\pm 12.5^\circ$ . Only those particles with less than 20 eV of kinetic energy are counted.

previously,<sup>10</sup> with a peak at  $\theta \approx 45\text{--}50^\circ$ . The C<sub>6</sub>H<sub>6</sub> molecule distribution peaks at  $\theta = 0^\circ$ . However tempting it is to fit this curve to a  $\cos^n \theta$  law, the exponent  $n$  cannot be uniquely determined since it depends on the polar angle resolution of the collection scheme.

**Molecular Orientation Effects: Benzene vs. Pyridine.** It is of interest to compare the ejection mechanisms for molecules bonded to the surface with different orientations. In benzene, the interaction with the surface is shared among six carbon atoms via the  $\pi$ -electron cloud. In pyridine, however, the bonding occurs almost totally through the nitrogen atom while the remainder of the molecule is pointing away from the surface. For comparison with the benzene calculations, 100 impacts are performed with 1000-eV Ar and the pyridine overlayer structure shown in Figure 1b. The most striking difference between the two cases is that the pyridine system exhibits almost complete lack of molecular ejection. This set of calculations produces only two C<sub>3</sub>NH<sub>3</sub> molecules and one NiC<sub>3</sub>NH<sub>3</sub> complex. There are, however, 23 diatomic (CH, NH) and 92 atomic (C, N, H) fragments. The CH/C<sub>6</sub> ratio is therefore much larger than for the benzene system. The reason for the major difference in fragmentation for these two structures is clear from an analysis of the three trajectories that led to molecular ejection of pyridine. Very simply, pyridine ejection requires the specific cleavage of a N–Ni bond during a single collision. When a carbon atom is struck, the molecule either stays on the surface or tends to dissociate. There appears to be no efficient modes of transferring the energy of collisions with the molecule into translation away from the surface. Obviously the original structure of the organic molecules, then, affects the ejection and fragmentation processes. One would not necessarily expect similar spectra from a sample of a monolayer of organic molecules on a metal, a liquid, or an ordered solid.

**Metal–Organic Clusters.** A variety of metal–organic clusters are observed to form and eject due to the collision cascade. The NiC<sub>6</sub>H<sub>6</sub> species is by far the most predominant although we also obtain NiC<sub>6</sub>H<sub>5</sub>, NiC<sub>n</sub>H<sub>n</sub>, with  $n \leq 5$ , and Ni<sub>2</sub>C<sub>6</sub>H<sub>6</sub> along with a few exotic species like Ni<sub>k</sub>(C<sub>6</sub>H<sub>6</sub>)<sub>2</sub>. It is almost impossible to make positive identification of these clusters since virtually nothing is known about their thermodynamic stabilities. The calculations predict, however, that the components are near each other in space and moving with small relative velocities.<sup>11</sup>

The calculations indicate that the Ni atom in the NiC<sub>6</sub>H<sub>6</sub> cluster is not necessarily originally underneath the adsorbed benzene molecule. Rather, there is a rearrangement involved in the formation of the metal–organic species. This mechanism is basically the same as found for the formation of NiCO and Ni<sub>2</sub>CO clusters.<sup>17</sup> The Ni atom and organic molecule eject and form a cluster in the near surface region. Because the two components must be close enough to experience bonding forces, the metal atom often

(35) S. P. Holland, B. J. Garrison, and N. Winograd, *Phys. Rev. Lett.*, **44**, 756 (1980).

(36) S. Kapur and B. J. Garrison, *J. Chem. Phys.*, **75**, 445 (1981); *Surf. Sci.*, **109**, 435 (1981).

originates from near the organic molecule on the surface. However, it is not possible to conclude that the Ni atom in a  $\text{NiC}_6\text{H}_6$  cluster was originally bound on the surface to the  $\text{C}_6\text{H}_6$  molecule.

The predicted energy distribution for the  $\text{NiC}_6\text{H}_6$  species exhibits a peak at a much higher energy than either the  $\text{C}_6\text{H}_6$  or Ni distributions (Figure 6a). This is characteristic of other clusters,  $\text{Cu}_2$  and  $\text{CuO}$ ,<sup>37</sup> which also form by this rearrangement process. These two component clusters form when each particle is moving with nearly the same velocity in a parallel direction. (Of course, they must be close enough together to be attracted to each other.) The peak in both the Ni and  $\text{C}_6\text{H}_6$  energy distributions occurs at approximately the same energy; thus since the masses are about equal, one would expect their velocity distributions to be nearly identical. For the  $\text{NiC}_6\text{H}_6$  cluster one also expects the velocity distribution to be similar, but since this species has twice the mass of the others, the peak in the energy distribution will occur at a higher energy as seen in Figure 6a.

Experimentally, it is observed that the energy distributions for both  $\text{Ni}^+$  and  $\text{NiC}_6\text{H}_6^+$  ions peak at  $\sim 2.5$  eV with the  $\text{NiC}_6\text{H}_6^+$  distribution terminating at  $\sim 12$  eV and the  $\text{Ni}^+$  distribution having a high-energy tail.<sup>9</sup> In a recent experimental and theoretical investigation of the energy and angular distributions of  $\text{Ni}^+$  and  $\text{NiCO}^+$  ions ejected from a CO-covered Ni(001) surface during ion bombardment, it was found that to obtain good agreement between the measured and calculated distributions the force experienced by ions due to the polarization of electrons in the metal must be taken into account.<sup>10</sup> This correction is applied to the calculated energy distribution with the results shown in Figure 6b. A value of 1.8 eV for the energy to overcome this image force yields the best fit between the experimental and calculated curves. The Ni and  $\text{NiC}_6\text{H}_6$  energy distributions are in quite good agreement with the experimental ones.

### Conclusions

The classical dynamics procedure has been used to model the desorption of organic molecules from metal surfaces due to collision cascades initiated by heavy particle bombardment. We find that this model predicts a mass spectrum and energy distributions similar to the experimental ones. For the system of a  $c(4 \times 4)$  overlayer of benzene on Ni(001), the mass spectrum is dominated by the parent species,  $\text{C}_6\text{H}_6$ , in the calculations and  $\text{NiC}_6\text{H}_6^+$  in the experiment. The internal energy of the ejected  $\text{C}_6\text{H}_6$  molecules is relatively low ( $\sim 75\%$  of the molecules have less than 5 eV of vibrational energy); thus we would predict that only a few of the molecules would fragment during the flight to the detector. The energy distributions for the Ni and  $\text{NiC}_6\text{H}_6$  species are similar to the experimental ones only if we take into account the image force that the ions would experience as they depart the surface.

The molecular ejection process is influenced by the bonding properties of the molecules to the substrate. For benzene, which is  $\pi$  bonded flat on the surface, we find considerable molecular desorption. There is virtually no molecular ejection, however, for pyridine, which  $\sigma$  bonds to the surface through the nitrogen lone pair. The mass spectrum then should reflect the initial bonding arrangement through the degree of fragmentation.

The reasons for the ejection of the intact molecules are threefold. (i) The collision energy of the final impact is generally reduced to tens of eV rather than  $\sim 1$  keV of the initial particle. (ii) The organic molecule has many degrees of vibrational freedom that can absorb excess energy without causing the molecule to fragment. (iii) The size of the carbon atoms is smaller than that of the nickel atom; thus the nickel atom can strike several carbon atoms simultaneously, pushing the whole molecule in one direction. We feel these mechanisms are extendable to molecules with higher molecular weights for two reasons. First, the molecular weight of a compound is not necessarily proportional to its size. For example, the diameter of a benzene molecule is  $\sim 5$  Å while the diameter of myoglobin with a mass of 16900 daltons is only  $\sim 35$  Å. Second, the size that is critical is the bonding cross section at the point of attachment. For example, a molecule 50-Å long but with a width of  $\sim 5$  Å would probably be easier to eject if it were standing up with only a small area of attachment rather than lying down where several bonds would have to be broken to remove it from the surface.

For clean metal and small molecule adsorption on metal studies we have found that the incident angle of the primary particle influences the ejection process. For polar angles of  $45^\circ$  for the incident Ar bombarding Cu(001), we find that considerably more shearing or peeling off of atoms occurs than for normal incidence.<sup>35,38</sup> Work is currently under way to examine the effect of off-normal angles of incidence to see if the molecular ejection can be enhanced. Finally, we feel that the fundamental processes involved in the nuclear motion of atoms due to heavy particle bombardment are well described by the classical dynamics procedure. These calculations should be equally applicable to either SIMS or FAB experiments.

**Acknowledgment.** We thank the National Science Foundation (Grant CHE-8022524) and the Office of Naval Research for financial support. We also acknowledge the A. P. Sloan Foundation for a Research Fellowship and the Camille and Henry Dreyfus Foundation for a grant for newly appointed young faculty. Professor Allinger was kind enough to send us the potential parameters used in his Molecular Mechanics II program. E. J. Karwacki provided his experimental results prior to publication.

Registry No.  $\text{C}_6\text{H}_6$ , 71-43-2; Ni, 7440-02-0.

(37) B. J. Garrison, N. Winograd, and D. E. Harrison, Jr., *Surf. Sci.*, **87**, 101 (1979).

(38) K. E. Foley and B. J. Garrison, *J. Chem. Phys.*, **72**, 1018 (1980).